Report

Current Biology

Predictive visuo-motor communication through neural oscillations

Graphical abstract

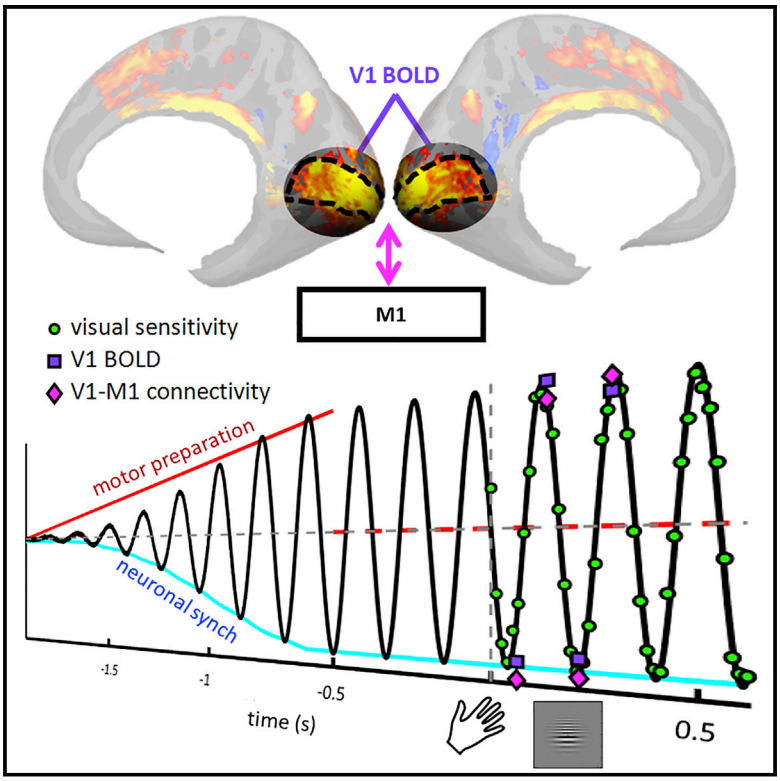

Authors

Alessandro Benedetto, Paola Binda, Mauro Costagli, Michela Tosetti, Maria Concetta Morrone

Correspondence

concetta.morrone@unipi.it

In brief

Benedetto et al. show that visual sensitivity, BOLD activity in primary visual cortex, and functional coupling between visual and motor cortex oscillate at the same theta frequency after a voluntary action. The results suggest that a motor preparation signal resets the phase of endogenous V1 rhythms to implement a flexible but precise coordination.

Highlights

- Visual evoked fMRI BOLD activity in V1 oscillates after a voluntary action
- The BOLD modulation in V1 follows the theta oscillation of visual sensitivity
- Enhanced coherence between motor and sensory cortex accounts for the oscillation
- Motor preparation predictively contributes to V1 processing of visual stimulation

Benedetto et al., 2021, Current Biology *31*, 1–8
August 9, 2021
https://doi.org/10.1016/j.cub.2021.05.026

CellPress

Please cite this article in press as: Benedetto et al., Predictive visuo-motor communication through neural oscillations, Current Biology (2021), https://doi.org/10.1016/j.cub.2021.05.026

Current Biology

CellPress
OPEN ACCESS

Report

Predictive visuo-motor communication through neural oscillations

Alessandro Benedetto,[1] Paola Binda,[1] Mauro Costagli,[2,3] Michela Tosetti,[3,4] and Maria Concetta Morrone[1,3,5,*]
[1]Department of Translational Research on New Technologies in Medicine and Surgery, University of Pisa, Pisa, Italy
[2]Department of Neuroscience, Rehabilitation, Ophthalmology, Genetics, Maternal and Child Sciences (DINOGMI), University of Genova, Genova, Italy
[3]Laboratory of Medical Physics and Magnetic Resonance, IRCCS Stella Maris, Pisa, Italy
[4]Imago 7 Research Foundation, Calambrone, Pisa, Italy
[5]Lead contact
*Correspondence: concetta.morrone@unipi.it
https://doi.org/10.1016/j.cub.2021.05.026

SUMMARY

The mechanisms coordinating action and perception over time are poorly understood. The sensory cortex needs to prepare for upcoming changes contingent on action, and this requires temporally precise communication that takes into account the variable delays between sensory and motor processing. Several theorists[1,2] have proposed synchronization of the endogenous oscillatory activity observed in most regions of the brain[3] as the basis for an efficient and flexible communication protocol between distal brain areas,[2,4] a concept known as "communication through coherence." Synchronization of endogenous oscillations[5,6] occurs after a salient sensory stimulus, such as a flash or a sound,[7–11] and after a voluntary action,[12–18] and this directly impacts perception, causing performance to oscillate rhythmically over time. Here we introduce a novel fMRI paradigm to probe the neural sources of oscillations, based on the concept of perturbative signals, which overcomes the low temporal resolution of BOLD signals. The assumption is that a synchronized endogenous rhythm will modulate cortical excitability rhythmically, which should be reflected in the BOLD responses to brief stimuli presented at different phases of the oscillation cycle. We record rhythmic oscillations of V1 BOLD synchronized by a simple voluntary action, in phase with behaviorally measured oscillations in visual sensitivity in the theta range. The functional connectivity between V1 and M1 also oscillates at the same rhythm. By demonstrating oscillatory temporal coupling between primary motor and sensory cortices, our results strongly implicate communication through coherence to achieve precise coordination and to encode sensory-motor timing.

RESULTS

Oscillation of behavioral sensitivity

Participants initiated each trial with a voluntary action (keypress), causing two grating patches of slightly different spatial frequency to appear above and below fixation, after a variable delay. Figure 1B shows spatial frequency discrimination performance averaged across all participants (Figures S1A–S1C show results for individual participants). Discrimination accuracy was not constant, but oscillated rhythmically over time, and is well fit by a sinusoidal function of 5.4 Hz (R^2 = 0.43, $p_{corrected}$ = 0.005; Figure 1B, inset). The first minimum in accuracy occurred 70 ms after action onset, consistent with "motor-induced suppression."[19] However, the suppression repeats periodically, generating an oscillatory pattern in the theta range, consistent with previous findings of behavioral oscillations synchronized with the onset of action.[12,14,17]

Oscillation of evoked BOLD responses in visual cortex

We repeated the psychophysical experiment of Figure 1A in an ultra-high magnetic field (7T) scanner, measuring the BOLD response evoked by a keypress followed by the visual grating. Given previous demonstrations that contrast sensitivity, known to reflect V1 activity, oscillates rhythmically after action onset,[14] we tested whether V1 activity is modulated by visuomotor delay by probing the peaks and the troughs of the accuracy oscillation. The BOLD response in V1 was strong and reliable, both when the stimuli were presented after the keypress action (vision and action; see activity map in Figure 1C) and when they were presented without the preceding keypress (vision only). However, the time courses of the two responses were qualitatively different (Figure 2A). For stimuli not preceded by action, the BOLD response followed the typical V1 hemodynamic (Figure 2A, black symbols); for stimuli preceded by the keypress action, the BOLD response reached a similar peak, but attenuated more rapidly (Figure 2A, blue-green symbols). This difference cannot be accounted for by a single multiplicative or additive factor (see Model of the BOLD visuo-motor response).

Figure 2B shows average hemodynamic responses separately for four stimulus delays (relative to keypress). The responses to stimuli presented at delays yielding minimal psychophysical accuracy (blue curves) were clearly less than to those at delays

Please cite this article in press as: Benedetto et al., Predictive visuo-motor communication through neural oscillations, Current Biology (2021), https://doi.org/10.1016/j.cub.2021.05.026

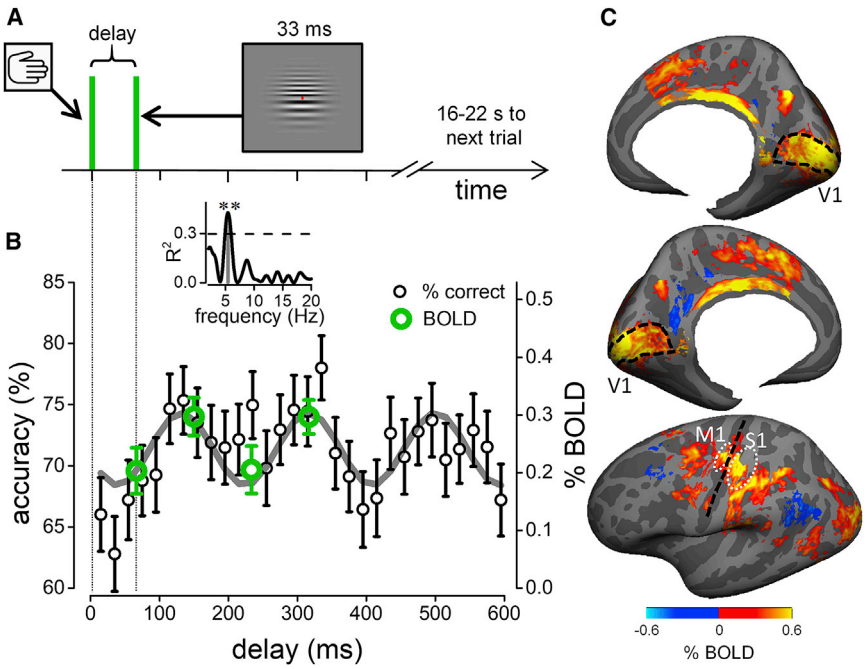

Figure 1. Experimental procedure and behavioral and BOLD responses

(A) Schematics of the behavioral and the time-resolved fMRI design, measuring responses to visual stimuli following a voluntary action. The delay between stimulus presentation and action onset varied randomly between 0 and 600 ms for the behavioral experiment, and randomly between four possible values (70, 150, 230, and 310 ms) for the fMRI experiment.

(B) Accuracy in the spatial frequency discrimination task as a function of visuo-motor delay (black symbols, mean and SEM; aggregate observer, n = 7), with the best sinusoidal fit of the accuracy time course (gray line; 5.4 Hz). Green circles show percent (%) BOLD signal change in V1 (integral of the hemodynamic response from 3 to 12 s divided by time) at the four visuo-motor delays tested (extracted from Figure 2C; mean and SEM; n = 17). Inset: goodness of the sinusoidal fit to the accuracy data in (B) as function of frequency, yielding a strong and significant peak at 5.4 Hz (R^2 = 0.43, $p_{correct}$ = 0.005) above the 95th percentile of the R^2 distribution obtained from fitting the permuted dataset with amplitude, phase, and frequency as free parameters to obtain a corrected p value.

(C) Maps of the BOLD response to vision and action events (estimated at 6 s) projected on a template of the cortical surface and aggregated across n = 17 participants; maps are masked at 0.05 significance after FDR correction. Black lines mark the central sulcus and V1 borders; white ovals mark the approximate surface location of the M1 and S1 ROIs.

See also Figure S1.

yielding maximal psychophysical accuracy (green curves). Figure 2C shows the average of the response over the interval of 3 to 12 s (integral divided by time). Responses at delays of 150 and 310 ms are significantly greater than at 70 and 230 ms. Repeated-measures ANOVA showed a significant effect of stimulus delay ($F(3,48) = 4.17$; $p = 0.01$; $\eta^2 = 0.21$), with amplitude at 70 and 230 ms significantly lower than the other two. The effect occurred in most of the 17 participants (Figure 2D). The BOLD rhythmic modulation between the combined peak versus the combined trough delays is significant from 6 s after action onset (Figure S2C, continuous line). In this analysis the BOLD regressors were aligned to the action onset, which produces massive responses in many motor and visual brain areas. However, similar visual BOLD modulations occurred when aligning the response to stimulus onset (Figures S2A–S2C, dashed line).

The V1 BOLD response amplitudes (Figure 1B, green circles) are highly consistent with the behavioral data collected outside the scanner, with the minima and the maxima of BOLD responses coinciding with the minima and maxima of performance in the spatial frequency discrimination task, confirming our hypothesis of a rhythmic modulation of V1 excitability.

BOLD correlations in the sensory-motor network

Having established that BOLD responses in V1 modulate rhythmically at around 5 Hz, we studied whether a similar oscillation also occurs in motor or somatosensory areas. For each participant, we defined ROIs in motor (M1) and somatosensory (S1) primary cortex using independent fMRI acquisitions and measuring the response to keypress used to report the perceptual decision (see ROIs in Figure S1D). The hemodynamic responses of M1 and S1 to vision and action events are different from those in V1 (compare Figure S2A to Figures S2D and S2G): the response occurred earlier (reflecting activity during action preparation[20]) and had a more pronounced negative lobe. However, the response was not modulated by the visuo-motor delay (Figures S2E and S2H) at any time of the hemodynamic response (Figures S2F and S2I), contrary to reported evidence when reaction times are also measured.[21]

The absence of M1 BOLD modulations with visual delay is consistent with the fact that motor cortex does not activate in response to visual stimuli. However, synchronous oscillatory activity may be present in M1 and shared with V1.[15] We used a correlation analysis to investigate this possibility. We subtracted the responses estimated independently at each time point and measured the shared trial-to-trial variability of BOLD residual signals between areas V1 and M1, obtaining a measure of functional connectivity. Figure 2E shows the correlation coefficients for the aggregate subject at each visuomotor delay; the correlation has an oscillatory pattern, with stronger correlations at delays of 150 and 310 ms. Similarly, a pairwise t test comparing correlations at the peak and trough delays across participants is statistically significant ($t(16) = 1.80$, $p = 0.044$). The correlation is strong and significant at all times (bootstrap of all trials of the aggregate subject: $p < 0.001$; one-sample t test across participants: all $t(16) > 3.5$, $p < 0.003$); however, and importantly, there was no modulation with delay for times preceding stimuli onset. The strongest increase in correlation occurred at +3 and +12 s, being about 20% (Figure 2F). This indicates that the increased correlations are not due to incomplete deconvolution of the signal, given that it is absent at 0 s and does not follow the hemodynamic response. Coupling between M1 and V1 is enhanced precisely at delays corresponding to maximum stimulus discriminability and BOLD V1 cortical excitability.

Please cite this article in press as: Benedetto et al., Predictive visuo-motor communication through neural oscillations, Current Biology (2021), https://doi.org/10.1016/j.cub.2021.05.026

CellPress
OPEN ACCESS

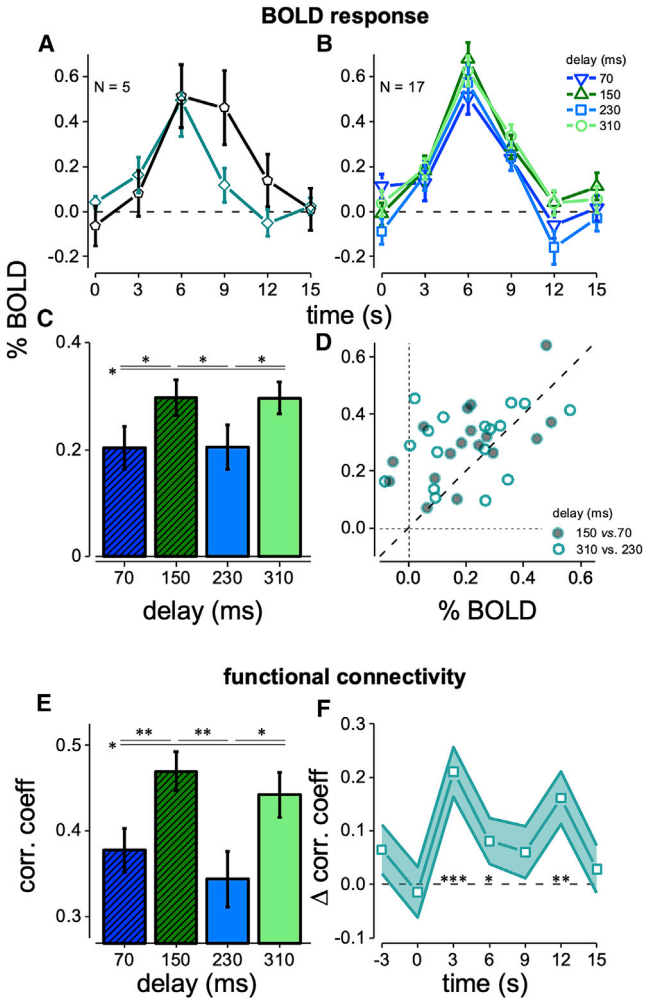

Figure 2. Oscillation of V1 BOLD responses and V1-M1 functional connectivity

(A) BOLD response (estimated as GLM beta weights using the finite impulse-response function deconvolution approach) for the V1 subregion representing the stimulus area; means and SEM from a subset of n = 5 participants in the vision-only (black curve) and vision and action condition (blue-green curve).

(B) Time course of the GLM beta weights (mean and SEM for all n = 17 participants) representing the BOLD response to vision and action events in the stimulated V1, separately for the 70, 150, 230, and 310 ms visuo-motor delays.

(C) Integral of the V1 response amplitude in the 3–12 s interval, divided by time, as function of visuo-motor delay. Asterisks mark statistical significance (0.05 > p > 0.01) of post hoc paired one-tailed t tests (Bonferroni-Holm corrected for multiple comparisons) comparing pairs of visuo-motor delays: 70 ms versus 150 ms, $t(16) = 2.88$, $p = 0.01$; 150 ms versus 230 ms, $t(16) = 2.54$, $p = 0.021$; 230 ms versus 310 ms, $t(16) = 2.20$, $p = 0.042$; 70 ms versus 310 ms, $t(16) = 2.33$, $p = 0.033$).

(D) V1 response amplitude in individual participants, plotting delay 150 ms against 70 ms (filled symbols) or delay 310 ms against 230 ms (empty symbols). The large majority of points lie above the bisection of the axes (dashed line) implying that V1 BOLD responses were higher for vision and action events associated with the peak of psychophysical performance, compared to those associated with the minima of performance.

(E) M1-V1 functional connectivity, estimated as the correlation coefficient between residuals of the GLM fit (integral between −3 and 12 s divided by time) and plotted as a function of visuo-motor delay. Bars show mean and SEM of the bootstrapped aggregate observer. Asterisks (here and other panels) indicate statistical significance: ns > 0.05 > *p > 0.01 > **p > 0.001 > ***p.

(F) Time course of the difference of the correlation coefficients of M1 and V1 residuals at the peak versus trough delays at each TR around the keypress action. Symbols and error bars are mean and SEM from the bootstrapped aggregate observer.

See also Figure S2.

Retinotopic dependence of rhythmic oscillation

The contrast map between BOLD responses for peak and trough delays (Figure S1E) shows that many areas of the occipital pole are modulated by visuo-motor delay. Consistent with the transient nature of the stimuli, BOLD activity at all delays is particularly strong in the V1/V2 region, with additional foci of activity in V3, V4, and parieto-occipital sulci (Figure 3A). It is clear on inspection that the effect of delay is prominent in V1: BOLD responses at 150 and 310 ms delays are stronger and more diffuse than at 70 or 230 ms. The effect of delay occurs at all V1 eccentricities (Figure 3B), even beyond the area covered by the stimulus (the bottom icon shows stimulus contrast across eccentricity). This implies that the effect of delay is independent of the stimulus characteristics, and probably driven by automatic and pervasive modulation of the excitability of the entire early visual cortex, which oscillates rhythmically in synchrony with action onset (see Model of the BOLD visuo-motor response).

Model of the BOLD visuo-motor response

The overall pattern of results strongly suggests that visual and motor cortices become synchronized during a simple visuo-motor task (keypress followed by a visual stimulus), and that the BOLD amplitude oscillates rhythmically with visuo-motor delay, suggesting that both cortices are driven by synchronization of endogenous oscillations. The salient findings are that (1) BOLD responses in V1 have a different time course when associated with a voluntary action (Figure 2A) and (2) the change of BOLD response with delay is not only multiplicative but includes an additive negative component (Figure 2B).

To capture both these effects, we developed a toy model simulating some well-known physiological properties of the visuo-motor loop, including corollary discharge signals during motor preparation that modulate V1, oscillatory rhythms, and gain modulation of visual responses (Figure 4A). The two key hypotheses are that (1) V1 activity is modulated in synchrony with motor signals, both before and after action, through phase synchronization of endogenous rhythms at theta frequency, and (2) the oscillation modulates V1 neuronal response gain.

We modeled the visual input with a delta function with amplitude chosen to maximize goodness of fit of V1 BOLD response to vision-only events, assuming a standard hemodynamic response[22] (black trace in the inset, $R^2 = 0.91$). To model the time course of the V1 BOLD response to vision and action events, we assumed that the visual input is combined with a motor preparation signal given by the "readiness potential," represented as a ramp signal starting 2 s before the action onset.[23,24] This readiness potential can also be recorded in V1 in the absence of visual stimulation (red curve in Figure 4B reporting the average activity in V1 in response to action-only events; see also Figure S1D maps), consistent with previous results.[25–28] Ramp amplitude in V1 was determined by the best fit of this response ($R^2 = 0.73$, amp = 0.27). As schematically illustrated in Figure S3A, the readiness potential is associated with (or may induce) network

Please cite this article in press as: Benedetto et al., Predictive visuo-motor communication through neural oscillations, Current Biology (2021), https://doi.org/10.1016/j.cub.2021.05.026

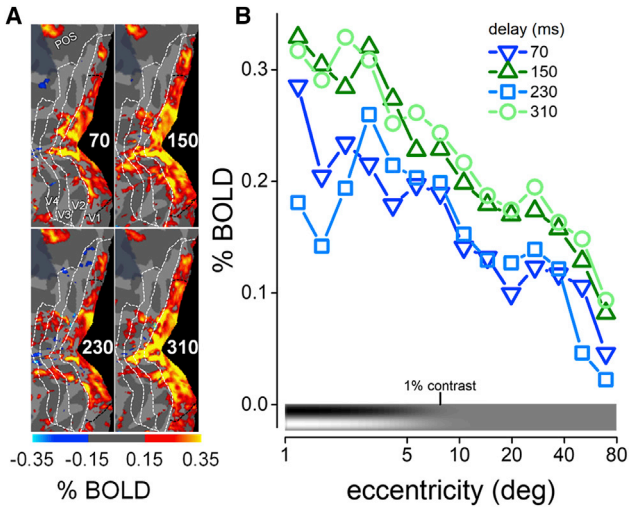

Figure 3. Effect of eccentricity on BOLD oscillations

(A) Maps of the posterior cortex response to vision and action events with the four visuomotor delays. BOLD responses were computed from the aggregate observer after projecting functional data from both hemispheres onto the mirror-symmetric template of the cortical surface. Maps are masked by the value of beta weights. White dashed lines indicate the borders between V1, V2, V3, and V4; dark dashed lines delimit the part of V1 stimulated by the gratings. The left panels show activity for the 70 and 230 ms visuo-motor delays, and the right panels for the 150 and 310 ms delays.

(B) V1 BOLD response (aggregate data, as shown in maps in A) plotted as function of eccentricity in 14 non-overlapping logarithmic steps from 1 to 80 deg. The icon by the x axis represents the variation of stimulus contrast over eccentricity.

oscillations at theta frequencies. The synchronization induces a negative and persistent signal, which we simulate over 4 s. The assumption of a negative signal is based on previous work showing that negative BOLD is associated with synchronized endogenous rhythms,[29,30] and with direct modeling of LFP and spiking activity associated with system dynamics.[31,32] The response to this negative signal, when summed with the responses to the motor preparation, predicted the M1 response (Figure S3D), and when summed with the visual stimulus predicted the time course of the response to vision and action events for delays at the troughs of the oscillation (Figure 4C, blue curve; $R^2 = 0.91$).

Finally, we postulated a small modulation of the gain of the visual response (estimated from the vision-only condition) following the theta rhythm after action onset (Figure S3A). This was achieved by moderate increase of the amplitude of the delta function that represents the visual input for the peak delay. A gain increase of about 33% is sufficient to fit the response to vision and action events for delays at the peak of the oscillation (Figure 4C, green trace; $R^2 = 0.92$). Both the subtractive signal and the gain modulation are consistent with neuronal mechanisms associated to the phase of synchronized oscillations in sensory cortex.[32]

With very few parameters, the model captures quantitatively the many different aspects of V1 and M1 BOLD modulations. The functional connectivity result (Figures 2E and 2F) can also be explained by synchronization of activity and common signals shared by M1 and V1 (Figure S3A) with their associated noise. The multiplicative response gain in V1 associated with the theta oscillations will contribute non-linearly to the co-variance between V1 and M1.[33] Numerical simulations (see Figure S3 caption) support this explanation.

DISCUSSION

Preparation of voluntary actions, such as finger-tapping, button-press, reaching, grasping, and even isometric muscle contraction, can modulate the perception of visual stimuli.[34] From hundreds of milliseconds before action onset (during motor preparation) to up to 1 s after action offset, visual sensitivity oscillates within the theta range, phase reset by action.[12,14,17] Here we found that V1 BOLD responses also oscillate at about 5 Hz following a voluntary action, strongly implicating V1 as the origin of the perceptual oscillation.

Although our paradigm did not allow us to correlate single-trial performance with BOLD responses to directly assess the link between BOLD oscillation and performance, our data, together with previous results from our laboratory,[11,12,14–17] show that the aggregate oscillations are consistent across the population. Furthermore, it is known that ERP during motor preparation can predict individual oscillatory performance.[15] Interestingly, the resolution of the delay-dependent BOLD modulation was finer than that required for humans to judge simultaneity between action onset and a visual stimulus (around 150 ms[35]), excluding cognitive effects. The BOLD V1 oscillation is also consistent with recordings in monkeys showing rhythmic theta-range modulation in V1.[36–38]

Our results provide strong evidence that voluntary action modulates V1 activity: not only was the visual response after a voluntary action different from that recorded during the vision-only condition, but a voluntary action on its own, unaccompanied by any visual stimulus, also elicited a significant V1 BOLD response. The observed pattern of V1 responses is consistent with the models of active sensing or embodied perception, which propose that processing of sensory inputs is profoundly altered when input is actively sought through eye, hand, or body movements, compared with passive stimulation.[39,40] Another well-described phenomenon associated with active sensing is motor-induced suppression of sensitivity, typically occurring in the first 100 ms after action onset. The phenomenon is very obvious after saccadic eye movements,[41] but also occurs after hand movements,[42,43] and can cause a measurable change in V1 BOLD response.[26] The attenuation of the response to stimulus presentation that we observe at 70 ms delay might be interpreted as the consequence of this motor inhibition. However, if this modulation of the hemodynamic response were simply transient motor suppression, we would have expected a monotonic increase with larger delays, rather than the rhythmic modulation we observe. Instead, our results point to a cyclic alternation starting before action onset. In this view, the function of the modulation is not to eliminate unstable sensory signals when sensors move, but rather is part of a cyclic mechanism of temporal binding.[1,2,4,34] The observed oscillation of BOLD responses and functional connectivity can be explained by synchronization of activity in motor and visual cortex by a common oscillatory rhythm present during the preparation phase. The anatomical pathways mediating

Please cite this article in press as: Benedetto et al., Predictive visuo-motor communication through neural oscillations, Current Biology (2021), https://doi.org/10.1016/j.cub.2021.05.026

CellPress
OPEN ACCESS

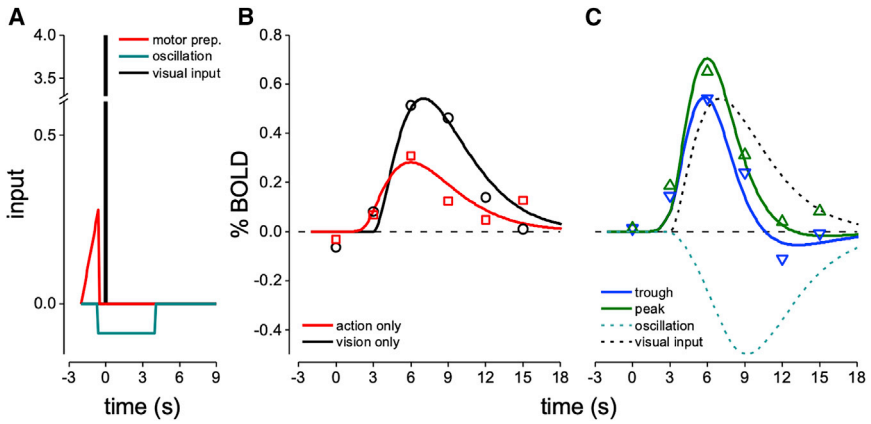

Figure 4. Simulation of V1 BOLD responses

(A) The model assumed three components: motor preparation modeled with a ramp function (in red, starting −2 s before and completed by −550 ms before action onset), neural oscillation as a negative boxcar (blue-green line, starting at −550 ms and completed 4 s after action onset), and visual input as a delta function (black line). Simulated curves in (B) and (C) were obtained by convolving the appropriately scaled inputs with a standard hemodynamic function[22] with decay time $\tau = 2$ s, order = 3, and delay $\delta = 3$ s.

(B and C) Simulated (lines) and observed (symbols) V1 BOLD responses to visual events presented without keypress (vision only, black curve in B and C), to keypress-only events (red curve in B and C), and to vision and action events associated with the trough (blue curve in C) or peak delays (green curve in C) of psychophysical performance.

See also Figure S3.

the synchronization are at present unknown; they may not require a direct input of M1 to V1 and they may involve subcortical, e.g., thalamic, relays.[44,45]

We modeled all the complex features of our results, including the perceptual modulation, by assuming that synchronous oscillations cause a general subtractive effect on BOLD signal in V1,[29–31] and that cortical excitability undergoes a multiplicative oscillatory gain change, which follows the phase of the theta rhythm.[32,36,37,46–48] Both our key assumptions are consistent with the BOLD literature.[49] Our data and model framework exploits a mechanism of "communication through coherence"[2] for transferring information between the sensory and the motor systems. This protocol is assumed to operate between distal cortical areas by synchronization of neural activity in local neuronal assemblies. Synchronized activity enhances effective connectivity within a local assembly and selectively improves the communication between assemblies.[2,4] Although synchronization typically occurs in the gamma range (30–90 Hz),[1,4] slower oscillations in the alpha and theta ranges can modulate the gamma rhythm and thereby affect communication.[36,37,46–48,50]

Other examples of communication through coherence exist in sensory-motor systems. Corticospinal gamma-band coherence occurs during movement preparation, and the coherence correlates with reaction times.[51] Functional connectivity between cortical areas changes depending on the local phase of the endogenous theta oscillation in humans.[52] Theta range synchronous modulation has been interpreted as a multiplexing mechanism to allocate processing resources to sensory and motor functions.[53] As with most multiplexing communication systems, this oscillatory communication may be efficient and easy to time-lock. Our results corroborate these findings, and together suggest an efficient, predictive, and flexible communication system through synchronization of endogenous rhythms for sensory-motor coordination. Flexibility is a critical issue, given that sensory-motor synchronization needs to rapidly recalibrate to accommodate internal and external changes (for example, fatigue can affect motor delays, and illumination visual delays). This complex task may become more manageable if time is encoded in a cyclical function, represented within primary sensory areas in the form of periodic modulations of cortical excitability.

Several studies propose that the phase of theta oscillations drives selective and spatial attention,[7,9,10,54–57] which are well known to modulate low-level areas such as V1.[58] Attention may in principle contribute to our results, but this seems unlikely for several reasons. First, the oscillation of V1 BOLD responses was not limited to the central visual field modulated by the stimulus, but extended to the far periphery of V1, which was neither stimulated nor task relevant. Second, V1 representations of upper and lower halves of the stimulus oscillated in-phase, consistent with evidence that oscillations synchronized by voluntary actions have the same phase across multiple locations,[12] whereas attentional fluctuations typically have opposite phases across locations.[7,9] Third, the V1 modulation was not stronger in the lower visual field, despite the lower-hemifield bias of attentional processes.[59] Another possibility is that oscillations of the rate of microsaccades or drift eye movements synchronized with keypress drive the rhythmic modulations reported here.[60,61] While we cannot dismiss this possible influence, in another study we measured microsaccade rate and found no correlation with the behavioral oscillation.[16]

Our results demonstrate that visuo-motor interactions have high temporal specificity, since perceptually indistinguishable changes in the delay between motor and visual events are sufficient to produce dramatic changes in the pattern of V1 activity, as well as of M1-V1 functional connectivity. Moreover, premotor signals (readiness potential) actively participate in the temporal recalibration of cortical activity necessary after adaptation to altered visuo-motor temporal delays for efficient processing.[62] All these examples may be interpreted as evidence for predictive coding of the future consequence of the action[1,42,43,63–68] elaborated during motor preparation and represented within sensory cortex. These predictions may be instrumental in stabilizing perception across movements, as well as in endowing a sense of agency.

Conclusion

The M1-V1 sensory-motor loop rhythmically oscillates at theta rhythm after a voluntary action, causing perceptual consequence such as modulation of visual sensitivity. The synchronized network dynamics may be instrumental for temporal

binding in the visuo-motor control system. This mechanism could underlie communication of the time of action from the motor cortex to the sensory cortex and encode it with high precision over the extended period when relevant sensory signals may arise.

STAR★METHODS

Detailed methods are provided in the online version of this paper and include the following:

- KEY RESOURCES TABLE
- RESOURCE AVAILABILITY
  - Lead Contact
  - Materials Availability
  - Data and Code Availability
- EXPERIMENTAL MODEL AND SUBJECT DETAILS
  - Human participants
- METHOD DETAILS
  - Behavioral experiment: setup and procedure
  - Behavioral oscillation analysis
  - fMRI experiment: setup and procedures
  - MRI scanning
  - Pre-processing of imaging data
- QUANTIFICATION AND STATISTICAL ANALYSIS
  - Definition of Regions of Interest (ROI)
  - Evaluation of fMRI Activity

SUPPLEMENTAL INFORMATION

Supplemental information can be found online at https://doi.org/10.1016/j.cub.2021.05.026.

ACKNOWLEDGMENTS

This project has received funding from the European Research Council (ERC) under the European Union's Horizon 2020 research and innovation programme (grant agreement no. 832813-GENPERCEPT and no. 801715-PUPILTRAITS) and by MIUR - PRIN 2017 grant 2017SBCPZY_02. We thank Eleanor Reynolds and David Burr for copyediting the manuscript. The authors would like to thank Dr. Brian Burns (GE Healthcare) for his implementation of the 3D-MP2RAGE sequence on the MR950 system.

AUTHOR CONTRIBUTIONS

Conceptualization, A.B., P.B., and M.C.M.; Methodology, all authors; Investigation, A.B., M.C.M., and P.B.; Writing, all authors.

DECLARATION OF INTERESTS

The authors declare no competing interests.

Received: February 25, 2021
Revised: April 22, 2021
Accepted: May 13, 2021
Published: June 9, 2021

REFERENCES

1. Engel, A.K., Fries, P., and Singer, W. (2001). Dynamic predictions: oscillations and synchrony in top-down processing. Nat. Rev. Neurosci. *2*, 704–716.
2. Fries, P. (2015). Rhythms for cognition: communication through coherence. Neuron *88*, 220–235.
3. Buzsáki, G. (2006). Rhythms of the Brain (Oxford University Press).
4. Womelsdorf, T., Schoffelen, J.M., Oostenveld, R., Singer, W., Desimone, R., Engel, A.K., and Fries, P. (2007). Modulation of neuronal interactions through neuronal synchronization. Science *316*, 1609–1612.
5. Busch, N.A., Dubois, J., and VanRullen, R. (2009). The phase of ongoing EEG oscillations predicts visual perception. J. Neurosci. *29*, 7869–7876.
6. VanRullen, R. (2016). Perceptual cycles. Trends Cogn. Sci. *20*, 723–735.
7. Landau, A.N., and Fries, P. (2012). Attention samples stimuli rhythmically. Curr. Biol. *22*, 1000–1004.
8. Romei, V., Gross, J., and Thut, G. (2012). Sounds reset rhythms of visual cortex and corresponding human visual perception. Curr. Biol. *22*, 807–813.
9. Fiebelkorn, I.C., Saalmann, Y.B., and Kastner, S. (2013). Rhythmic sampling within and between objects despite sustained attention at a cued location. Curr. Biol. *23*, 2553–2558.
10. Song, K., Meng, M., Chen, L., Zhou, K., and Luo, H. (2014). Behavioral oscillations in attention: rhythmic α pulses mediated through θ band. J. Neurosci. *34*, 4837–4844.
11. Ho, H.T., Leung, J., Burr, D.C., Alais, D., and Morrone, M.C. (2017). Auditory sensitivity and decision criteria oscillate at different frequencies separately for the two ears. Curr. Biol. *27*, 3643–3649.e3.
12. Tomassini, A., Spinelli, D., Jacono, M., Sandini, G., and Morrone, M.C. (2015). Rhythmic oscillations of visual contrast sensitivity synchronized with action. J. Neurosci. *35*, 7019–7029.
13. Wutz, A., Muschter, E., van Koningsbruggen, M.G., Weisz, N., and Melcher, D. (2016). Temporal integration windows in neural processing and perception aligned to saccadic eye movements. Curr. Biol. *26*, 1659–1668.
14. Benedetto, A., Spinelli, D., and Morrone, M.C. (2016). Rhythmic modulation of visual contrast discrimination triggered by action. Proc. Biol. Sci. *283*, 20160692.
15. Tomassini, A., Ambrogioni, L., Medendorp, W.P., and Maris, E. (2017). Theta oscillations locked to intended actions rhythmically modulate perception. eLife *6*, e25618.
16. Benedetto, A., and Morrone, M.C. (2017). Saccadic suppression is embedded within extended oscillatory modulation of sensitivity. J. Neurosci. *37*, 3661–3670.
17. Zhang, H., Morrone, M.C., and Alais, D. (2019). Behavioural oscillations in visual orientation discrimination reveal distinct modulation rates for both sensitivity and response bias. Sci. Rep. *9*, 1115.
18. Assaneo, M.F., Rimmele, J.M., Sanz Perl, Y., and Poeppel, D. (2021). Speaking rhythmically can shape hearing. Nat. Hum. Behav. *5*, 71–82.
19. Aliu, S.O., Houde, J.F., and Nagarajan, S.S. (2009). Motor-induced suppression of the auditory cortex. J. Cogn. Neurosci. *21*, 791–802.
20. Cunnington, R., Windischberger, C., Deecke, L., and Moser, E. (2003). The preparation and readiness for voluntary movement: a high-field event-related fMRI study of the Bereitschafts-BOLD response. Neuroimage *20*, 404–412.
21. Guo, B., Lu, Z., Goold, J.E., Luo, H., and Meng, M. (2020). Fluctuations of fMRI activation patterns in visual object priming. Human Behaviour and Brain *1*, 78–84.
22. Boynton, G.M., Engel, S.A., Glover, G.H., and Heeger, D.J. (1996). Linear systems analysis of functional magnetic resonance imaging in human V1. J. Neurosci. *16*, 4207–4221.
23. Libet, B., Gleason, C.A., Wright, E.W., and Pearl, D.K. (1983). Time of conscious intention to act in relation to onset of cerebral activity (readiness-potential). The unconscious initiation of a freely voluntary act. Brain *106*, 623–642.
24. Shibasaki, H., and Hallett, M. (2006). What is the Bereitschaftspotential? Clin. Neurophysiol. *117*, 2341–2356.
25. Gutteling, T.P., Petridou, N., Dumoulin, S.O., Harvey, B.M., Aarnoutse, E.J., Kenemans, J.L., and Neggers, S.F. (2015). Action preparation shapes processing in early visual cortex. J. Neurosci. *35*, 6472–6480.

26. Straube, B., van Kemenade, B.M., Arikan, B.E., Fiehler, K., Leube, D.T., Harris, L.R., and Kircher, T. (2017). Predicting the multisensory consequences of one's own action: BOLD suppression in auditory and visual cortices. PLoS ONE *12*, e0169131.
27. Gallivan, J.P., Chapman, C.S., Gale, D.J., Flanagan, J.R., and Culham, J.C. (2019). Selective modulation of early visual cortical activity by movement intention. Cereb. Cortex *29*, 4662–4678.
28. Monaco, S., Malfatti, G., Culham, J.C., Cattaneo, L., and Turella, L. (2020). Decoding motor imagery and action planning in the early visual cortex: overlapping but distinct neural mechanisms. Neuroimage *218*, 116981.
29. Becker, R., Reinacher, M., Freyer, F., Villringer, A., and Ritter, P. (2011). How ongoing neuronal oscillations account for evoked fMRI variability. J. Neurosci. *31*, 11016–11027.
30. Scheeringa, R., Fries, P., Petersson, K.M., Oostenveld, R., Grothe, I., Norris, D.G., Hagoort, P., and Bastiaansen, M.C. (2011). Neuronal dynamics underlying high- and low-frequency EEG oscillations contribute independently to the human BOLD signal. Neuron *69*, 572–583.
31. Magri, C., Schridde, U., Murayama, Y., Panzeri, S., and Logothetis, N.K. (2012). The amplitude and timing of the BOLD signal reflects the relationship between local field potential power at different frequencies. J. Neurosci. *32*, 1395–1407.
32. Kayser, C., Wilson, C., Safaai, H., Sakata, S., and Panzeri, S. (2015). Rhythmic auditory cortex activity at multiple timescales shapes stimulus-response gain and background firing. J. Neurosci. *35*, 7750–7762.
33. Goris, R.L., Movshon, J.A., and Simoncelli, E.P. (2014). Partitioning neuronal variability. Nat. Neurosci. *17*, 858–865.
34. Benedetto, A., Morrone, M.C., and Tomassini, A. (2020). The common rhythm of action and perception. J. Cogn. Neurosci. *32*, 187–200.
35. Stetson, C., Cui, X., Montague, P.R., and Eagleman, D.M. (2006). Motor-sensory recalibration leads to an illusory reversal of action and sensation. Neuron *51*, 651–659.
36. Bosman, C.A., Schoffelen, J.M., Brunet, N., Oostenveld, R., Bastos, A.M., Womelsdorf, T., Rubehn, B., Stieglitz, T., De Weerd, P., and Fries, P. (2012). Attentional stimulus selection through selective synchronization between monkey visual areas. Neuron *75*, 875–888.
37. Spyropoulos, G., Bosman, C.A., and Fries, P. (2018). A theta rhythm in macaque visual cortex and its attentional modulation. Proc. Natl. Acad. Sci. USA *115*, E5614–E5623.
38. Kienitz, R., Cox, M.A., Dougherty, K., Saunders, R.C., Schmiedt, J.T., Leopold, D.A., Maier, A., and Schmid, M.C. (2021). Theta, but not gamma oscillations in area V4 depend on input from primary visual cortex. Curr. Biol. *31*, 635–642.e3.
39. Ballard, D.H. (1991). Animate vision. Artif. Intell. *48*, 57–86.
40. Harman, K.L., Humphrey, G.K., and Goodale, M.A. (1999). Active manual control of object views facilitates visual recognition. Curr. Biol. *9*, 1315–1318.
41. Burr, D.C., Morrone, M.C., and Ross, J. (1994). Selective suppression of the magnocellular visual pathway during saccadic eye movements. Nature *371*, 511–513.
42. Wolpert, D.M., Ghahramani, Z., and Jordan, M.I. (1995). An internal model for sensorimotor integration. Science *269*, 1880–1882.
43. Blakemore, S.J., Wolpert, D.M., and Frith, C.D. (1998). Central cancellation of self-produced tickle sensation. Nat. Neurosci. *1*, 635–640.
44. Wurtz, R.H. (2018). Corollary discharge contributions to perceptual continuity across saccades. Annu. Rev. Vis. Sci. *4*, 215–237.
45. Fiebelkorn, I.C., Pinsk, M.A., and Kastner, S. (2019). The mediodorsal pulvinar coordinates the macaque fronto-parietal network during rhythmic spatial attention. Nat. Commun. *10*, 215.
46. Canolty, R.T., Edwards, E., Dalal, S.S., Soltani, M., Nagarajan, S.S., Kirsch, H.E., Berger, M.S., Barbaro, N.M., and Knight, R.T. (2006). High gamma power is phase-locked to theta oscillations in human neocortex. Science *313*, 1626–1628.
47. Landau, A.N., Schreyer, H.M., van Pelt, S., and Fries, P. (2015). Distributed attention is implemented through theta-rhythmic gamma modulation. Curr. Biol. *25*, 2332–2337.
48. Helfrich, R.F., Fiebelkorn, I.C., Szczepanski, S.M., Lin, J.J., Parvizi, J., Knight, R.T., and Kastner, S. (2018). Neural mechanisms of sustained attention are rhythmic. Neuron *99*, 854–865.e5.
49. Scheeringa, R., and Fries, P. (2019). Cortical layers, rhythms and BOLD signals. Neuroimage *197*, 689–698.
50. Haegens, S., Nácher, V., Luna, R., Romo, R., and Jensen, O. (2011). α-Oscillations in the monkey sensorimotor network influence discrimination performance by rhythmical inhibition of neuronal spiking. Proc. Natl. Acad. Sci. USA *108*, 19377–19382.
51. Schoffelen, J.M., Oostenveld, R., and Fries, P. (2005). Neuronal coherence as a mechanism of effective corticospinal interaction. Science *308*, 111–113.
52. Hanslmayr, S., Volberg, G., Wimber, M., Dalal, S.S., and Greenlee, M.W. (2013). Prestimulus oscillatory phase at 7 Hz gates cortical information flow and visual perception. Curr. Biol. *23*, 2273–2278.
53. Fiebelkorn, I.C., and Kastner, S. (2019). A rhythmic theory of attention. Trends Cogn. Sci. *23*, 87–101.
54. Huang, Y., Chen, L., and Luo, H. (2015). Behavioral oscillation in priming: competing perceptual predictions conveyed in alternating theta-band rhythms. J. Neurosci. *35*, 2830–2837.
55. Jia, J., Liu, L., Fang, F., and Luo, H. (2017). Sequential sampling of visual objects during sustained attention. PLoS Biol. *15*, e2001903.
56. Mo, C., Lu, J., Wu, B., Jia, J., Luo, H., and Fang, F. (2019). Competing rhythmic neural representations of orientations during concurrent attention to multiple orientation features. Nat. Commun. *10*, 5264.
57. Re, D., Inbar, M., Richter, C.G., and Landau, A.N. (2019). Feature-based attention samples stimuli rhythmically. Curr. Biol. *29*, 693–699.e4.
58. Carrasco, M. (2011). Visual attention: the past 25 years. Vision Res. *51*, 1484–1525.
59. He, S., Cavanagh, P., and Intriligator, J. (1996). Attentional resolution and the locus of visual awareness. Nature *383*, 334–337.
60. Martinez-Conde, S., Otero-Millan, J., and Macknik, S.L. (2013). The impact of microsaccades on vision: towards a unified theory of saccadic function. Nat. Rev. Neurosci. *14*, 83–96.
61. Melloni, L., Schwiedrzik, C.M., Rodriguez, E., and Singer, W. (2009). (Micro)saccades, corollary activity and cortical oscillations. Trends Cogn. Sci. *13*, 239–245.
62. Cai, C., Ogawa, K., Kochiyama, T., Tanaka, H., and Imamizu, H. (2018). Temporal recalibration of motor and visual potentials in lag adaptation in voluntary movement. Neuroimage *172*, 654–662.
63. Rao, R.P., and Ballard, D.H. (1999). Predictive coding in the visual cortex: a functional interpretation of some extra-classical receptive-field effects. Nat. Neurosci. *2*, 79–87.
64. Friston, K. (2005). A theory of cortical responses. Philos. Trans. R. Soc. Lond. B Biol. Sci. *360*, 815–836.
65. Schroeder, C.E., Wilson, D.A., Radman, T., Scharfman, H., and Lakatos, P. (2010). Dynamics of active sensing and perceptual selection. Curr. Opin. Neurobiol. *20*, 172–176.
66. Arnal, L.H., and Giraud, A.L. (2012). Cortical oscillations and sensory predictions. Trends Cogn. Sci. *16*, 390–398.
67. Brown, H., Adams, R.A., Parees, I., Edwards, M., and Friston, K. (2013). Active inference, sensory attenuation and illusions. Cogn. Process. *14*, 411–427.
68. Friston, K.J., Bastos, A.M., Pinotsis, D., and Litvak, V. (2015). LFP and oscillations-what do they tell us? Curr. Opin. Neurobiol. *31*, 1–6.
69. Fischl, B. (2012). FreeSurfer. Neuroimage *62*, 774–781.
70. Goebel, R. (2012). BrainVoyager–past, present, future. Neuroimage *62*, 748–756.
71. Jenkinson, M., Beckmann, C.F., Behrens, T.E., Woolrich, M.W., and Smith, S.M. (2012). Fsl. Neuroimage *62*, 782–790.

72. Ashburner, J. (2012). SPM: a history. Neuroimage *62*, 791–800.

73. Brainard, D.H. (1997). The Psychophysics Toolbox. Spat. Vis. *10*, 433–436.

74. Benedetto, A., Burr, D.C., and Morrone, M.C. (2018). Perceptual oscillation of audiovisual time simultaneity. eNeuro *5*, ENEURO.0047-18.2018.

75. Costagli, M., Ueno, K., Sun, P., Gardner, J.L., Wan, X., Ricciardi, E., Pietrini, P., Tanaka, K., and Cheng, K. (2014). Functional signalers of changes in visual stimuli: cortical responses to increments and decrements in motion coherence. Cereb. Cortex *24*, 110–118.

76. Benson, N.C., Butt, O.H., Datta, R., Radoeva, P.D., Brainard, D.H., and Aguirre, G.K. (2012). The retinotopic organization of striate cortex is well predicted by surface topology. Curr. Biol. *22*, 2081–2085.

Please cite this article in press as: Benedetto et al., Predictive visuo-motor communication through neural oscillations, Current Biology (2021), https://doi.org/10.1016/j.cub.2021.05.026

CellPress
OPEN ACCESS

STAR★METHODS

KEY RESOURCES TABLE

REAGENT or RESOURCE	SOURCE	IDENTIFIER
Software and algorithms		
MATLAB r2010a, r2020b	MathWorks	http://www.mathworks.com/products/matlab/; RRID: SCR_001622
Freesurfer v6.0.0	[69]	http://surfer.nmr.mgh.harvard.edu/; RRID: SCR_001847
BrainVoyager 20.6	[70]	http://www.brainvoyager.com/products/brainvoyagerqx.html; RRID: SCR_013057
FSL v5.0.10	[71]	http://www.fmrib.ox.ac.uk/fsl/; RRID: SCR_002823
SPM12	[72]	http://www.fil.ion.ucl.ac.uk/spm/; RRID: SCR_007037
Psychophysics Toolbox v3	[73]	http://psychtoolbox.org/; RRID: SCR_002881

RESOURCE AVAILABILITY

Lead Contact

Further information and requests for resources should be directed to the Lead Contact, Maria Concetta Morrone (concetta.morrone@unipi.it).

Materials Availability

This study did not generate new unique reagents.

Data and Code Availability

Analyses were performed with Freesurfer v6.0.0, SPM12, BrainVoyager 20.6, and FSL (version 5.0.10) packages and MATLAB (version R2020b). BOLD map activity, matrices of residuals of V1 and M1, as well as a summary of the behavioral/BOLD results presented in the figures have been deposited to Mendeley Data: https://doi.org/10.17632/nbxkb9xxr8.1.

EXPERIMENTAL MODEL AND SUBJECT DETAILS

Human participants

Experimental procedures are in line with the declaration of Helsinki and were approved by the regional ethics committee (*Comitato Etico Pediatrico Regionale—Azienda Ospedaliero-Universitaria Meyer*—Firenze (FI)) and by the Italian Ministry of Health, under the protocol '*Plasticità e multimodalità delle prime aree visive: studio in risonanza magnetica a campo ultra-alto (7T)*' version #1 dated 11/11/2015. Written informed consent was obtained from each participant, which included consent to process and preserve the data and publish them in anonymous form.

We recruited seven participants for the behavioral experiment (26-36 years old, mean age = 30, 3 females and 4 males), with normal or corrected to normal vision. Twenty-four healthy participants with normal or corrected-to-normal vision were recruited for the fMRI experiment. Three of them did not complete the scanning session and were excluded from the analyses. Of the remaining 21 participants (24-63 years old, mean age = 30, 9 females and 12 males), 17 took part in the main experiment that included 60 ± 17 visual presentations over 5 ± 2.5 fMRI acquisition series (mean ± SD).

METHOD DETAILS

Behavioral experiment: setup and procedure

Behavioral measurements were made in a quiet room in dim light condition. The stimuli were generated in MATLAB (MATLAB r2010a; MathWorks), displayed with a graphics board ViSaGe (Cambridge Research System) on a linearized CRT monitor (Barco Calibrator 40 × 30cm, resolution of 800 × 600pxl, refresh rate 100Hz, mean luminance 25cd/m^2) at 57cm from the observer. Keypress responses were acquired by CB6 response box (Cambridge Research System) with a negligible estimated time error < 1ms (as per manufacturer's specifications). Stimulus presentation was synchronized with the monitor framerate, implying that visuo-motor synchronization could be determined with an error between −10 and +0ms.

The visual stimulus comprised two horizontal gratings (10% contrast, spatial frequency 1c/° and 1.1c/°) presented for 30ms (3 frames) in the upper and lower visual field, both vignetted by a Gaussian window (σ = 5°) at screen center (see inset Figure 1). The two gratings were separated by a Gaussian horizontal blank with space constant of 0.5° (σ). The two gratings were presented

Please cite this article in press as: Benedetto et al., Predictive visuo-motor communication through neural oscillations, Current Biology (2021), https://doi.org/10.1016/j.cub.2021.05.026

randomly between to top and the bottom field with each trial. The phase of each grating also varied randomly across trials. Participants maintained fixation on a small red dot (0.15°) at the center of the display and pressed a key to start the trial (with the fourth finger of the right hand). The visual stimulus was displayed at 60 possible stimulus delays (corresponding from 1 to 60 monitor frames) from button press, chosen randomly on each trial from a uniform distribution between 0 and 600ms in steps of 10ms. The participant's task was to indicate which grating (upper or lower) had the higher spatial frequency (i.e., a 2AFC spatial frequency discrimination task) by pressing a button with the index or the middle finger of the right hand.

Participants were instructed to wait at least 1 s between two successive keypresses (this interval was 1.6 s on average, with 1 s standard deviation). Trials with an ITI of less than 1 s (1.3% of trials) were excluded from further analysis. We collected on average 1008 ± 187 trials for each participant.

Behavioral oscillation analysis

To test whether visual accuracy fluctuated rhythmically over time, we pooled all trials from all participants (aggregate subject), sorted them in terms of visuo-motor delays and grouped them into 20ms non-overlapping bins (but note the duration of the stimulus, 30ms). For each bin, we computed the proportion of correct responses and fitted the resulting time series with the following sine function:

$$y(x) = \beta_0 + \beta_1 \sin(2\pi f x) + \beta_2 \cos(2\pi f x), \quad \text{(Equation 1)}$$

where f represents the frequency of the oscillation and can vary between 2 and 20Hz in steps of 0.1Hz; β_0, β_1 and β_2 are free parameters to be estimated. Statistical significance was evaluated by comparing the goodness of fit (R^2) for the original dataset, with the distribution of goodness of fits obtained on permuted datasets created by shuffling the original responses (10000 permutations). For each permutation, we selected the best fitting sinusoidal model, with frequency, amplitude and phase free parameters and compared the distribution of the obtained R^2 with the R^2 of the real data best fit. To use all free parameters for the fit of surrogate data allows to correct automatically for multiple comparisons of the frequency range.

To evaluate the consistency of amplitude and phase across subjects, we ran multivariable generalized linear model (GLM) applied to single-trial response.[15,74] For each participant, we fitted a linear regression model including as predictors a sine and a cosine for a given frequency of interest (between 3.5 and 10Hz, resolution of 0.1Hz). The fixed-effect linear regression parameters were estimated using standard least square method (LSM). The beta coefficients of the participants were tested against 0 by means of the bivariate Hotelling's T-squared statistic, i.e., an extension of the Student's t test to the multivariate domain.

fMRI experiment: setup and procedures

Visual stimuli were presented by using a magnetic resonance-compatible goggle set (VisuaStimDigital, Resonance Technologies, Northridge, California) with visual field of approximately 32 × 24°, 800 × 600 resolution, refresh rate 60Hz (16.7ms frame), mean luminance 25cd/m^2. Keypresses were recorded through a magnetic resonance-compatible response-box (Evoke Response Pad System, Resonance Technologies, Northridge, California), positioned on the right hand of volunteers. The time of the keypress was recorded with a constant error of 10 ± 0.5ms, (due to the MS Windows software) and associated with the time-stamp of the frame in which it occurred.

The same visual stimulus and procedure of the behavioral experiment were used in the fMRI scans, with the following differences. To accommodate for the different refresh rate of the monitor, the duration of the stimulus was limited to two frames (33ms). The high sensitivity of 7T fMRI allowed for recording reliable BOLD responses to such brief stimulus, even for small numbers of events. Stimulus presentations were synchronized with the monitor framerate, implying that visuo-motor synchronization could be determined with an error between −10 and +6ms (slightly asymmetric due to the constant delay of the keypress time-stamp). As for the behavioral experiment, participants started the trial by pressing a key using the fourth finger (chosen based on the high sensitivity of the key). They were instructed to wait at least 15 s between two successive keypresses. The subject practice the task before entering the scanner till they reach a correct timing pace without using an internal count-down.

In the main experiment, the task was to silently perform the spatial-frequency discrimination task and to report an estimate of the average proportion of "up" responses at the end of each acquisition series.

In a small set of runs (not included in the main analyses), all 21 participants were required to report perceptual decisions with a second keypress, delayed by several seconds (15 s on average, with 4 s standard deviation) to minimize interference with the visual presentation. These trials were used to assess stimulus discriminability in the scanner and to check that performance was not saturated at 100% correct or at 50% correct. These trials were used to assess stimulus discriminability in the scanner; while most participants performed well above chance with an average 62 ± 3% correct, few of them (5 out 17) complained that maintaining an accurate memory of the choice for so long time was very hard and performed near chance (below 54%). Excluding these participants brought average performance to 69%, very similar as in the behavioral experiment conducted outside the scanner ($t(11) = 0.56$, $p = 0.581$, considering the full population the t test was $t(16) = 2.45$, $p = 0.027$) . The paucity of trials across all participants did not allow for tracking oscillations in accuracy as function of visuo-motor asynchrony; this also prevented us from analyzing the single-trial correlation between BOLD and behavioral responses.

For each participant we used the BOLD modulation associated with the decision keypress to locate cortical areas holding a representation of the keypress action both in M1 and S1 (Figure S1). Primary visual cortex V1 was localized by separate retinotopic mapping data (two 45° wedges centered around the horizontal or vertical meridian, presented alternately for 5TRs each, with no blanks, and six repetitions in total for a total of 12TRs).

Please cite this article in press as: Benedetto et al., Predictive visuo-motor communication through neural oscillations, Current Biology (2021), https://doi.org/10.1016/j.cub.2021.05.026

Data for the main experiment (with no keypresses for perceptual decisions) were collected in 17 of the 21 subjects. Visual stimuli were presented every 19 s on average (3 s standard deviation) at 4 asynchronies between the keypress and the visual stimulus (delay = 70, 150, 230, or 310ms, with the −10:+6 error range indicated above); keypresses (and the following visual presentations) could not be aligned with the TR since participants pressed the key at their own pace; each acquisition series lasted 130TR of 3 s. The average number of trials (±1 standard deviation) per participant were: 17 ± 6 for delay 70ms; 17 ± 6 for delay 150ms; 13 ± 5 for delay 230ms; 13 ± 4 for delays 310ms (privileging shorter delays that were perceptually indistinguishable[35]). In order to define the design matrix used for the GLM analyses, we assigned each *vision and action* event to the TR preceding action onset. This meant that in about 3% of trials, the visual presentation actually occurred 1TR later than indicated in the design matrix (this happened in about 5% of trials for the 310ms delay, and 4%, 3%, and 2% for the 230, 150 and 70ms delays respectively). We verified that aligning the design matrix to the visual stimulus rather than the action onset did not change the results (Figures S2A and S2B). We also verified that the temporal distribution of events was homogeneous in the TR, using circular statistics (Rayleigh test for 70ms delays: $p = 0.34$; 150ms delays: $p = 0.55$; 230ms: $p = 0.89$; 310ms delays: $p = 0.45$). The results ensured that there were no temporal biases between conditions and therefore that event timing could not explain response amplitude differences. Given the limitations in scanning time at 7T (about 1 h per subject per 6 months), testing was limited to 4 delays that matched the maxima and minima of psychophysical performance; this logically corresponds to testing the hypothesis that BOLD responses had the same oscillations as psychophysical performance.

Finally, we ran a feasibility experiment testing a subset of N = 5 participants with vision-only events, where the visual stimulus onset was delivered by keypress performed by the experimenter (average number of trials ± 1 standard deviation per participant: 13 ± 0.5). The subject reported silently the task as in the main experiment. Also in this condition the timing of the visual presentation was jittered relative to the TR; circular statistics verified that the temporal distribution of events was homogeneous in the TR (Rayleigh test: $p = 0.24$).

MRI scanning

Scanning was performed on a MR950 7T whole body MRI system (GE Healthcare, Milwaukee, WI, USA) equipped with a 2-channel transmit coil driven in quadrature mode, a 32-channel receive coil (Nova Medical, Wilmington, MA, USA) and a high-performance gradient system (50mT/m maximum amplitude and 200mT/m/ms slew rate).

For twelve participants, the anatomical images were acquired at 1mm isotropic resolution using a T1-weighted magnetization-prepared Fast Spoiled Gradient Echo (FSPGR) sequence with the following parameters: TR = 6ms, TE = 2.2ms, flip angle = 12°, receiver Bandwidth = 50kHz, TI = 450ms, ASSET = 2. For the remaining 9 participants, high-resolution anatomical images with 0.8mm isotropic resolution were acquired with a modified magnetization-prepared rapid gradient echo sequence (MP2RAGE) with the following parameters: TR = 6.6ms, TE = 2.5ms, flip angle = 5°, receiver Bandwidth = 62.5kHz, TI = 1000ms and 3200ms, ARC factor = 2.

Functional images were acquired with a gradient-echo EPI sequence with slices N = 46 (with an ascending interleaved order), Field of View = 192mm, matrix size = 128x128, resulting in a spatial resolution of 1.5x1.5mm^2 in-plane, and slice thickness 1.4mm with slice spacing = 0.1mm, TR = 3 s, TE = 23ms, flip angle = 60°, receiver Bandwidth = 250kHz, ASSET acceleration factor = 2, phase encoding direction: Anterior-to-Posterior. No resampling was performed during the reconstruction. For each EPI sequence, we acquired an additional volume with the reversed phase encoding direction (Posterior-to-Anterior), used for distortion correction (see Pre-processing of imaging data).

Pre-processing of imaging data

Anatomical images were processed by a standard procedure for segmentation implemented in Freesurfer (recon-all). In addition, hemispheres were aligned to a template of the cortical surface (fsaverage) as well as to the left/right symmetric version of the same template (fsaverage_sym).

We used Brain Voyager with default settings to perform slice time correction and motion correction. Geometrical distortions were compensated by using EPI images with reversed phase encoding direction (Brain Voyager COPE plug-in). The pre-processed images were aligned to each participant's anatomical image using a boundary-based registration algorithm (Freesurfer "*bbregister*" algorithm) and projected to the cortical surface of each hemisphere. All analyses were conducted on data in the individual subject space, resampled to a resolution of 3x3x3mm. For each run, we removed the first 6TRs (to allow the MR signal to reach steady-state), then estimated the temporal linear trend and subtracted it from the fMRI time-course. Time-courses were averaged within each ROI (see below) and converted into percentage signal change by normalizing them to the mean BOLD.

QUANTIFICATION AND STATISTICAL ANALYSIS

Definition of Regions of Interest (ROI)

For each participant, we defined three ROIs (bilateral V1, left M1 and left S1) in the 3D native space of each participant. V1 was defined using the responses to the vertical and horizontal meridians from the retinotopic mapping scans and included the cortical representation of the stimulus area, in both hemispheres of about 7.3cm^3. The M1 and S1 ROIs were defined based on the pattern

Please cite this article in press as: Benedetto et al., Predictive visuo-motor communication through neural oscillations, Current Biology (2021), https://doi.org/10.1016/j.cub.2021.05.026

of BOLD responses to keypress associated with the perceptual decision that generated two separate foci located rostrally and caudally of the left Rolandic sulcus, consistent with M1 and Brodmann Area 3a. The M1 and S1 ROIs comprised on average 5.8cm^3 of cortex.

Evaluation of fMRI Activity

We used the Finite Impulse Response deconvolution approach for estimating the Hemodynamic Response Function (HRF) over a window of 7TRs following each event (an ''event'' being a visual stimulus presentation, a voluntary keypress or both). This analysis approach does not assume a particular shape of the hemodynamic response but, rather, estimates it directly by modeling each of the 7TRs after the events as a separate GLM predictor and thereby assigning each with a beta-weight.[75] Given that visual stimuli and the keypress that started the trial were separated by less than 350ms, we aligned the predictor with the TR that included the keypress (Figure S2A shows V1 BOLD responses computed after aligning to the visual stimulus instead: compare Figure S2A with Figure 2A in the main text). In each ROI, seven beta values per each event type were estimated with GLM (e.g., for the main analyses, we considered four types of events corresponding to the 4 visuo-motor delays, making 28 predictors to which we added a constant term); the average goodness of fit was 20 ± 2% (average number of time points: 629).

Statistical comparisons were performed after extracting GLM beta-weights in individual participants and in each of our *a priori* defined ROIs.

We assessed pairwise correlations between M1 and V1 in the aggregate observer data, after regressing out the event-related modulations, i.e., using the residuals of the GLM model. Specifically, we performed 4 steps: 1) compute the predicted time-course given the estimated GLM weights for each run; 2) subtract it from the observed time-course to obtain the residuals; 3) concatenate residuals from all runs and all participants; 4) compute the Pearson's correlation between residuals in the two ROIs. Correlation coefficients were then averaged in the −3 to 12 s interval around vision and action events, separately for the four visuomotor delays. Correlation differences across delays were assessed by bootstrap (10000 repetitions with replacement, one-tailed test), repeating step #4 10000 times for each delay. We complemented this aggregate subject analysis with a more standard repeated-measures approach, where correlations were computed for each participant and visuomotor delay. Correlation differences across delays were then assessed with paired t tests.

GLM beta weights at the TRs of interest (the peak of hemodynamic response at TR2 for Figures 1C and S1D, or the integral of beta weights (divided by time) from TR1 to TR4 for Figures 3 and S1D) were also visualized over a template of the cortical surface. These were estimated after projecting the pre-processed BOLD time courses from each participant on a common template, concatenating them and then applying the GLM analysis. For Figures 1C, S1D, and S1E, data from the two hemispheres were analyzed separately; for Figure 3, a mirror-symmetric template of the cortical surface was used and the concatenated BOLD time courses were averaged across hemispheres before the GLM analysis. Except for Figure 3A, activity maps were masked for statistical significance ($p_{FDR} < 0.05$, Figure S1E reports uncorrected p values). Eccentricities in primary visual cortex were defined according to the Benson template for fsaverage.[76]

Current Biology, Volume *31*

Supplemental Information

Predictive visuo-motor communication through neural oscillations

Alessandro Benedetto, Paola Binda, Mauro Costagli, Michela Tosetti, and Maria Concetta Morrone

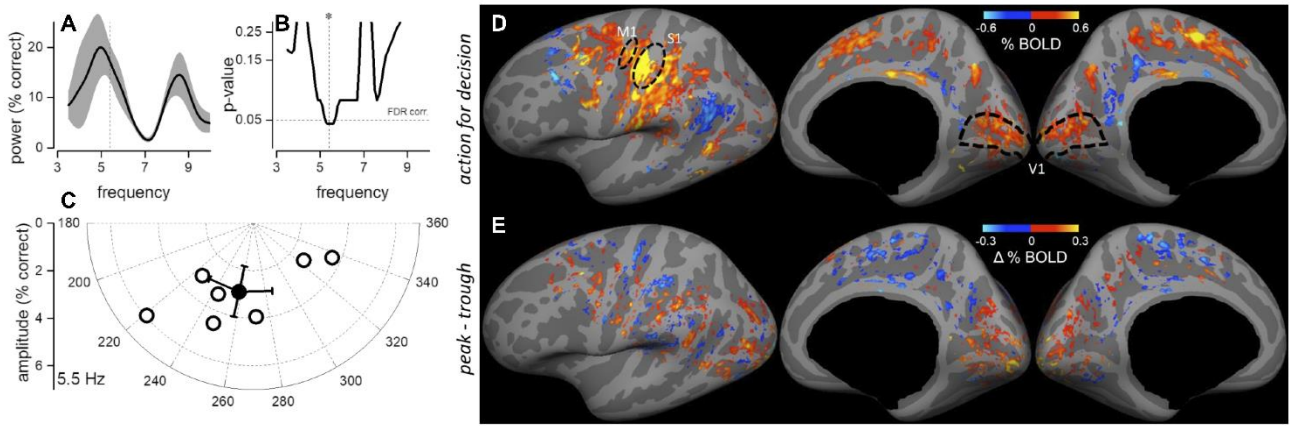

Figure S1. Behavioural and BOLD responses. Related to Figure 1.

A-C: consistency of perceptual oscillation across participants, obtained by fitting each participant's dataset with sinusoidal curves. **A:** Power and s.e.m averaged across participants as a function of frequencies between 3.5 and 10 Hz. **B:** FDR-corrected statistical significance, derived from Hotelling T^2 distribution across participants, which is maximal at 5.5 Hz, very similar to the best fit for the mean power across participants. **C.** Amplitude and phase of the best fitting of a sinusoidal function at 5.5 Hz in each participant, clearly clustered around 260°. The filled circle plots mean amplitude and phase with s.e.m.

D: Maps of the BOLD response to *action-only* events, measured in an independent set of trials where participants performed the 2AFC task. The activity is related to the keypress reporting the perceptual decision (separated by at least 15s from any *vision and action* event). BOLD activity is estimated as the peak of the haemodynamic, at 6s, and masked at 0.05 significance after FDR correction. Activity around the central sulcus of the left hemisphere defined the M1 and S1 ROI (in each participant's volume; black lines mark the approximate projection of these ROIs). Other foci of activity included the early visual cortex, which was strongly and unexpectedly modulated with *action-only* events, putative area V6 in the parieto-occipital[S1, S2] sulcus as well as portions of the cingulate cortex[S2], both similarly active in response to *vision and action* events (compare with Figure 1C of the main text).

E: Contrast of the BOLD response to *vision and action* events at SOAs corresponding to the peak vs. trough delays of psychophysical performance, masked at 0.05 significance uncorrected and computed as the integral from 3 to 12 s of the haemodynamic response, divided by time. Positive modulations clustered in the occipital lobe; there was no clear positive or negative modulation in the other foci of activity for the vision and action events (see Figure 1C in the main text): neither putative area V6 in the parieto-occipital sulcus, nor the cingulate sulcus visual area or the somatosensory and motor areas show consistent clustering of contrast values.

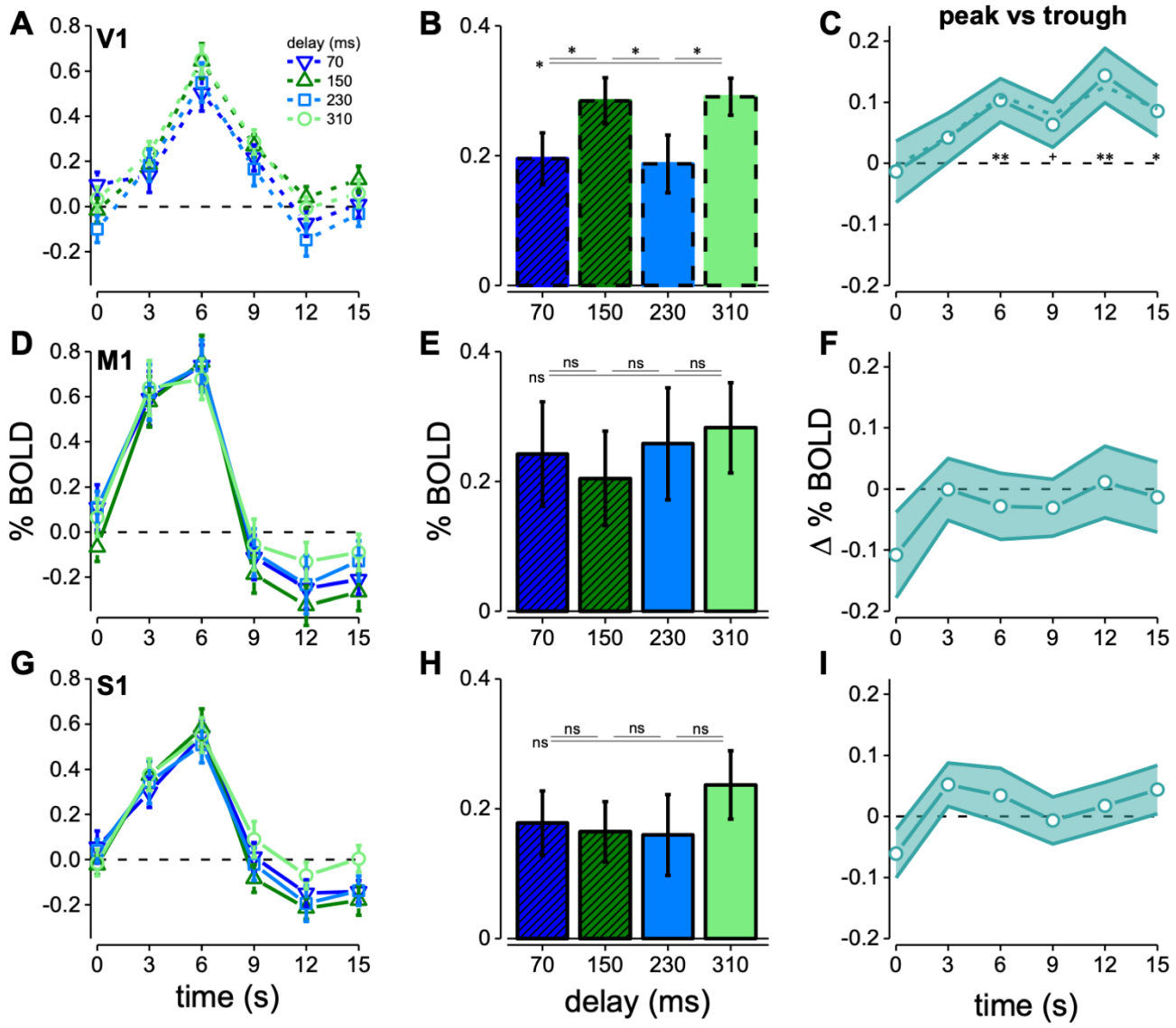

Figure S2. V1, M1 and S1 BOLD responses to *vision and action* events. Related to Figure 2.

A-B. same as B-C in Figure 2 of the main text, but with GLM beta weights for the V1 BOLD response estimated after aligning data to the onset of the visual stimulus, rather than to the keypress action. Asterisks in B mark statistical significance (0.05 > * > 0.01) of post-hoc paired one-tailed t-tests (Bonferroni-Holm corrected for multiple comparisons) comparing pairs of visuo-motor delays: 70 ms vs 150 ms: $t(16) = 2.69$, $p = 0.032$; 150 ms vs 230 ms: $t(16) = 2.64$, $p = 0.032$; 230 ms vs 310 ms: $t(16) = 2.47$, $p = 0.026$; 70 ms vs 310 ms: $t(16) = 2.45$, $p = 0.025$).

C. Modulation of the V1 response to vision and action events associated with the peak vs. trough delays of psychophysical performance, computed for each TR following the keypress action (continuous lines) or the stimulus (dashed lines). For the continuous line, statistical significance is for TRs: 0 s: $t(16) = 0.27$, $p = 0.60$; 3 s: $t(16) = 1.04$, $p = 0.15$; 6 s: $t(16) = 2.90$, $p = 0.005$; 9 s: $t(16) = 1.70$, $p = 0.054$; 12 s: $t(16) = 3.23$, $p = 0.002$; 15 s: $t(16) = 2.04$, $p = 0.028$ (p: 0.06 > + > 0.05 > * > 0.01 > ** > 0.001).

D-I. BOLD response for vision and action events associated with the peak vs. trough delays of psychophysical performance in M1 (D, E, F) or S1 (G, H, I). No comparisons reach significant threshold ($p<0.16$, uncorrected).

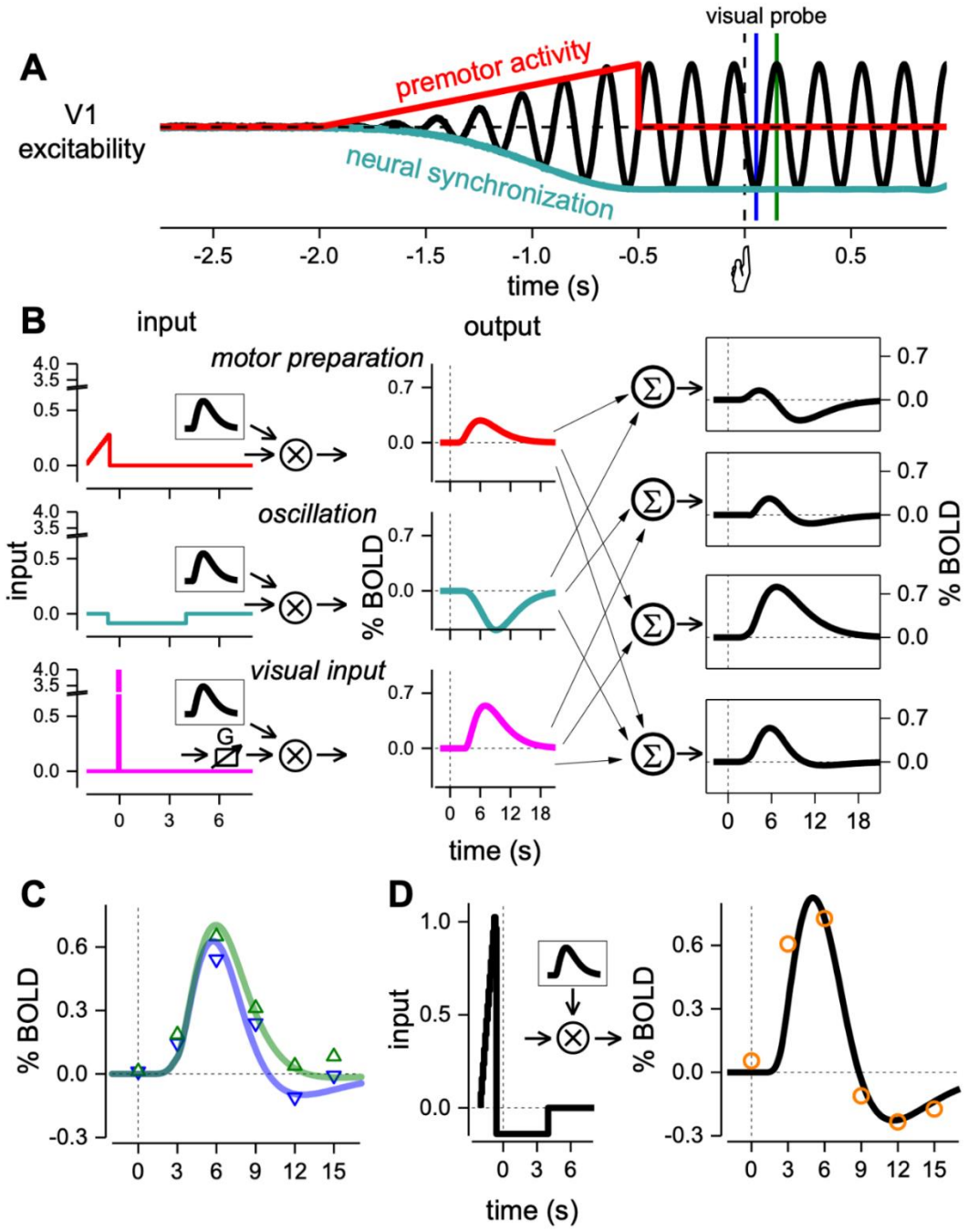

Figure S3. Simulation of the V1 and M1 BOLD response and their functional connectivity. related to Figure 4.

A. We assume that the neural activity underlying BOLD responses to *vision and action* events can be described with the following components: 1) a ramp preceding the action and representing premotor activity, e.g. in the form of a readiness potential (red curve; onset −2 s, offset −0.55 s from action onset); and 2) an oscillatory signal, generated by the phase synchronization of endogenous rhythms around 5.4 Hz (black curve), which reaches maximum amplitude before the action onset and persists for several seconds after (from −0.55 s to +4 s; schematically represented by the black curve). We further assume that V1 response gain is dynamically modulated by the oscillatory signal, implying that responses to identical visual stimuli are more enhanced when presented at the peak of the oscillation (green line) then when presented at the trough (blue line).

B,C,D. To simulate the BOLD response, the above signals are convolved with the standard model of the haemodynamic response given by:

$$IRF(t) = \frac{\left(\frac{t-\delta}{\tau}\right)^{(n-1)} e^{-\left(\frac{t-\delta}{\tau}\right)}}{\tau(n-1)!}$$

[eq. S1]

With decay time $\tau = 2s$, delay $\delta = 3s$, and order $n = 3$.

To keep model complexity low, the visual response is modelled by a delta function, and pre-motor activity is the same as in A. The synchronization of endogenous oscillations has been simulated with a negative constant signal (blue-green curve), given previous evidence that oscillatory phase coherence of endogenous rhythms is associated with negative BOLD[S3, S4]. The visual response amplitude changes with delay to simulate the action of gain (G) set by the synchronization.

Different combinations of the three inputs, after convolution with the *IRF(t)*, fit the different BOLD responses. The amplitude of the ramp was set to 0.27 by best fit (R^2 =0.74) of the V1 BOLD response to *action-only* events (see maps in Figure S1 and Figure 4 red curve).

The amplitude of the delta function was set to 4 by best fitting (R^2=0.91) the response of the *vision-only* response (Figure 2A, pink curve). These values were then used as fixed parameters in the fit of the BOLD response in V1 as a function of delay.

The timing of the offset of the ramp and onset of the negative signals were set to −550 ms by best fitting of the data of the M1 responses as shown in D. The best fit of M1 (R^2=0.89) was obtained with ramp amplitude equal to 1.10 and negative component equal to 0.13.

Any linear combination of the BOLD response to the ramp (first row in panel B) and delta functions (third row in panel B) will be inadequate to fit the M1 or V1 BOLD response to *vision and action* events, given the slow decay of the sum (third panel of the left column, in B) and the lack of a negative lobe. However, the linear combination of these two signals is necessary to reproduce the fast growth of the visual response in the first two TR (6 s) to *vision and action* compared to the *vision-only* events (compare dashed black curve with blue curve in Figure 4C). To model the response to *vision and action* of V1, it was necessary to add the negative signal. The result adequately fit (R^2=0.92) the response to *vision and action* for the trough delays (blue curve or Figure 4C, blue curve) using an amplitude of the constant signal equal to −0.08. To fit adequately the peak delay responses, which differ from the trough especially for the reduced negative lobe, it is necessary to change the ratio between amplitude of response and amplitude of negative BOLD.

A good fit was obtained by modulating the gain of the visual response by a factor of 1.3 (Figure 4C). The alternative strategy of reducing the negative signal amplitude also allows fitting of the response to trough delays, obtaining an R^2 value of 0.88, lower than increasing the gain equal to 0.92 (Figure S3,C). In addition, a reduction of negative signal is difficult to explain given that this signal is present before the presentation of the visual stimulus. Both gain modulation and constant signal have been shown to be important to simulate how LFP in sensory cortex changes with synchronization of rhythms[S5].

Gain modulation may also be crucial to explain the variation of functional connectivity between M1 and V1 with delay. Single cell recordings have demonstrated that correlation between neurons can be modelled considering that the total variance of the discharge is weighted by the gain variance[S6]. To test if similar mechanisms can be applied for BOLD functional connectivity, we simulated the modulation of V1 visual response by M1 noise given by:

$$V1_{out}(t) = \alpha \cdot \big(IRF(t) \otimes S(t)\big) \cdot N_{M1}(t) + N_{V1}(t)$$

[eq. S2]

and

$$M1(t) = N_{M1}(t)$$

[eq. S3]

where $IRF(t)$ is the neuronal impulse response function estimated by the Gamma function of equation S1 with a time decay τ =80 ms, $\delta = 15ms$ and order n of 2; $N_{M1}$and $N_{V1}$are white noise of specific amplitude and free parameter variance. S is a series of about 16 events randomly positioned in a time interval of 300 s.

We applied to $V1_{out}$ the same GLM adopting the same finite IRF approach used for our analyses with 60 equi-spaced regressors in time separated by 10 ms. We verified that the GLM produced unbiased estimates of the visual response in V1 (despite the presence of a non-linearity), and that the residuals did not contain IRF(t) information. The correlation between V1 and M1 (for time window containing the first 200 ms of IRF duration) increased as a function of gain increase (α). Enhancing excitability in V1 by a factor of 1.3 (the same factor used to model the visual responses in Figure 4C) increased the V1-M1 correlation by about 1.27. The parameter to achieve a modulation that fits well the data of Figure 2E were N_{V1}, a white noise in the range [0:0.4], $N_{M1}$is a motor noise in the range [0:0.1], α is equal to 2. Convolving $V1_{out}$ and *M1* of equations S2 and S3 with the haemodynamic function of equation S1, and repeating the procedure increased correlation but did not change the modulation with visuo-motor delay. The simulation reinforces the concept that gain modulation may be a key mechanism for functional coupling of distal brain regions.

Supplemental references:

S1. Pitzalis, S., Sereno, M.I., Committeri, G., Fattori, P., Galati, G., Patria, F., and Galletti, C. (2010). Human V6: The Medial Motion Area. Cerebral Cortex *20*, 411-424.

S2. Smith, A.T., Beer, A.L., Furlan, M., and Mars, R.B. (2018). Connectivity of the Cingulate Sulcus Visual Area (CSv) in the Human Cerebral Cortex. Cerebral Cortex *28*, 713-725.

S3. Scheeringa, R., Fries, P., Petersson, K.M., Oostenveld, R., Grothe, I., Norris, D.G., Hagoort, P., and Bastiaansen, M.C. (2011). Neuronal dynamics underlying high- and low-frequency EEG oscillations contribute independently to the human BOLD signal. Neuron *69*, 572-583.

S4. Magri, C., Schridde, U., Murayama, Y., Panzeri, S., and Logothetis, N.K. (2012). The Amplitude and Timing of the BOLD Signal Reflects the Relationship between Local Field Potential Power at Different Frequencies. Journal of Neuroscience *32*, 1395-1407.

S5. Kayser, C., Wilson, C., Safaai, H., Sakata, S., and Panzeri, S. (2015). Rhythmic Auditory Cortex Activity at Multiple Timescales Shapes Stimulus-Response Gain and Background Firing. Journal of Neuroscience *35*, 7750-7762.

S6. Goris, R.L., Movshon, J.A., and Simoncelli, E.P. (2014). Partitioning neuronal variability. Nat Neurosci *17*, 858-865.